JCTC Journal of Chemical Theory and Computation

pubs.acs.org/JCTC Article

Quantum Chemistry Density Matrix Renormalization Group in the Discrete Variable Representation

Bing Gu,* Jiajun Ren, and Junzhe Zhang

Cite This: J. Chem. Theory Comput. 2025, 21, 6793−6800 Read Online

ACCESS | Metrics & More | Article Recommendations

ABSTRACT: We present a numerical implementation of the quantum chemistry density matrix renormalization group (DMRG) using the hybrid discrete variable representation (DVR)/Gaussian basis set. The z-axis of real space is discretized by a DVR basis set and each transversal plane is described by the eigenstates of the transversal core Hamiltonian, represented in a set of primitive Gaussian basis functions. Such a hybrid basis can reduce the computation of two-electron repulsion integrals. One main advantage of using the local DVR basis sets over finite-difference methods for real space discretization is that the kinetic energy operator matrix elements can be computed exactly. This method is first applied to a one-dimensional pseudo-hydrogen chain under screened Coulomb potential and then to a realistic hydrogen chain, whereby the DMRG/DVR results are comparable in accuracy to the full configuration interaction results.

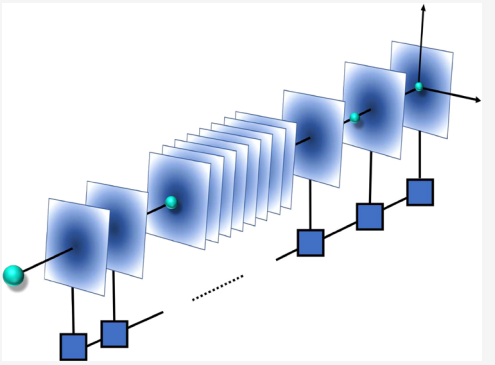

1. INTRODUCTION

Electronic structure is the cornerstone of modern chemistry and is now routinely performed for molecules and materials to understand their physicochemical properties and spectroscopy.[1,2] Most of the electronic structure codes employ Gaussian-type orbitals as the atomic integrals can be analytically computed. The two-electron integrals are fundamental components required for any electronic structure computations,[3] e.g., to construct the Fock matrix in the Hartree−Fock (HF) method. The evaluation of electron repulsion integrals is computationally demanding as it scales N^4 with the size of the basis set N. Real-space grids provide an alternative universal basis set for electronic structure computations.[4−11]

The discrete variable representation (DVR) basis set using both a finite number of basis functions and a set of grid points, has been widely used in solving the molecular vibrational eigenstates problems[12−18] as it simplifies the computations of both kinetic energy and potential energy operator matrix elements. However, much less is explored to use DVR basis sets for electronic structure computations, especially in advanced multiconfigurational methods.[7,19] The main difficulty with DVR basis sets in electronic structure comes from the Coulomb singularities, this occurs even for a single hydrogen atom. Previous attempts employing DVR set in electronic structure computations typically uses a soft Coulomb potential.[7,19]

Here we present an implementation of the quantum chemistry density matrix renormalization group (DMRG) using a hybrid contracted Gaussian/DVR basis sets (sliced basis). We avoid the Coulomb singularities by using DVR in only one or two dimensions while using Gaussian basis functions for the remaining axes. DMRG is a numerical method developed to study quantum many-body systems, particularly in one-dimensional systems. Originally introduced by White,[20] it has become one of the most powerful computational methods in condensed matter physics and, more recently, in quantum chemistry for calculating ground state and low-lying excited states of molecules.[21−23] DMRG represents many-electron states using matrix product states, composed of interconnected tensors with a restricted entanglement. While conventionally the quantum chemistry DMRG uses the canonical molecular orbitals as sites, using a localized basis set as DMRG sites can enhance its performance by reducing the entanglement.[24] Specifically, the sliced basis DMRG uses a real-space grid for z coordinate, while the transversal plane uses Gaussian basis sets.[24] The kinetic energy operator is computed approximately by a finite-difference method, which requires a dense uniform grid to have good accuracy; see refs 25,26 for more recent developments of DMRG with wavelet transformed Gaussians (so-called gausslet). Here we use DVR basis sets for the z-discretization such that the one- and two-electron integrals can be computed easily with high accuracy. The DVR basis sets are rooted in the

Received: January 9, 2025
Revised: May 28, 2025
Accepted: May 30, 2025
Published: July 2, 2025

https://doi.org/10.1021/acs.jctc.5c00029
J. Chem. Theory Comput. 2025, 21, 6793−6800

numerical quadrature and share the properties of locality and orthogonality with the gausslets. The transversal orbitals are constructed by solving the eigenstates of the transversal core Hamiltonian, retaining fewer eigenstates than the number of primitive basis functions. The parameters for the primitive transversal Gaussian basis functions are extracted from standard basis sets. Besides locality, another advantage of using such hybrid Gaussian/real-space basis set is the electron repulsion integral scales, instead of $O(N^4)$ using Gaussian-type orbitals, as $O(N_z^2 N_o^4)$, where N_z is the number of slices and N_o is the number of transversal orbitals for each slice. In general, the required number of transversal orbitals is much smaller than the number of canonical molecular orbitals $N_o \ll N$. In our construction of the transversal basis functions (see Sec. II), the scaling can be further reduced to $O(N_z N_o^4)$ for chain molecules because the primitive transversal Gaussian basis functions are the same for each slice.

We first apply our method to a one-dimensional pseudo-hydrogen chain with screened Coulomb potential, where the DVR set is expected to have better convergence with the number of grid points. For this 1D model system, we also implemented the complete active space configuration interaction (CASCI) method employing the same DVR basis sets, with the complete active space defined by the HF canonical molecular orbitals. CASCI includes all possible electronic configurations (Slater determinants) by distributing electrons among the active orbitals.[27] Unlike the complete active space self-consistent field, the active orbitals are predetermined, e.g., canonical HF molecular orbitals. It is shown that the DMRG energy with a very small bond dimension $D \sim 10$ matches the CASCI energy up to 10^{-4} E_h. We then apply our method to a realistic hydrogen chain, H_n. As the DVR basis set has not been implemented in standard electronic structure methods for realistic molecules, here we compare our results with CCSD (coupled cluster singles and doubles) and FCI (full configuration interaction) using conventional Pople basis set to benchmark the accuracy. It is shown that the DMRG/DVR energies with primitive Gaussians extracted from STO-6G is lower than the FCI/6−31G energies. All codes are implemented in our in-house Python-based package PyQED, the matrix product state-based implementations are based on the package Renormalizer.[28]

This paper is organized as follows. In Section 2, we present the method of DMRG in a DVR basis set and then describe the implementation details. The applications to a one-dimensional pseudo-hydrogen chain model and to the realistic hydrogen chain is shown in Section 3. We discuss the challenges and future perspectives of DVR basis sets in Section 4.

Atomic units $\hbar = e = m_e = 1$ are used throughout.

2. METHOD

2.1. DVR Basis Set. The DVR basis sets consist of a projection operator $\hat{P}$, usually defined by a finite number of basis functions $\hat{P} = \sum_{n=1}^{N} |u_n\rangle\langle u_n|$, where $\{|u_n\rangle\}$ is an orthonormal set, and a set of grid points $\{x_i\}$, not necessarily uniform.[12,16] The DVR basis functions are obtained from the projected position eigenstates corresponding to the grid points (i.e., Dirac δ function $\langle x|x_i\rangle = \delta(x - x_i)$),

$$|\Delta_i\rangle = \hat{P}|x_i\rangle \tag{1}$$

It immediately follows that[16]

$$\langle \Delta_i|\Delta_j\rangle = \langle x_i|\Delta_j\rangle = \langle \Delta_i|x_j\rangle \tag{2}$$

Introducing the normalized states $|\phi_i\rangle = w_i^{-1/2}|\Delta_i\rangle$, $w_i = \langle \Delta_i|\Delta_i\rangle$, if they satisfy the following property

$$\langle x_j|\phi_k\rangle = w_j^{1/2}\delta_{jk} \tag{3}$$

they define a DVR set. Equations 3 and 2 imply the orthonormality of a DVR set

$$\langle \phi_i|\phi_j\rangle = \delta_{ij} \tag{4}$$

There are many kinds of DVR sets such as the sinc functions, Gauss−Hermite DVR, and particle-in-a-box eigenstates (i.e., sine functions).[12,16,17] The optimal choice depends on the specific problem and the boundary conditions. One example is the so-called sinc DVR

$$\phi_i(x) = \frac{1}{\sqrt{\Delta x}}\mathrm{sinc}(\pi(x - x_i)/\Delta x) \tag{5}$$

where the grid points are $x_i = x_0 + i\Delta x$, $i = 0, \pm 1, \pm 2, \cdots$ and Δx is the grid spacing, corresponding to a projection operator of band-limited functions $\hat{P} = \int_{-\Lambda}^{\Lambda} dp|p\rangle\langle p|$, where $\Lambda = \pi/\Delta x$ is the momentum cutoff. In practice, the infinite sinc functions have to be truncated. The advantage of a DVR is the highly localized character of the basis functions about the grid points. Thus, only a small number of functions is required to represent a spatially localized electronic orbital.

The DVR basis functions are approximately the eigenstates of the projected position operator $X = \hat{P}\hat{x}\hat{P}$. To see this, applying the projection operator to $\hat{x}|x_i\rangle = \hat{x}(\hat{P} + \hat{Q})|x_i\rangle = \hat{x}(\hat{P}^2 + \hat{Q})|x_i\rangle = x_i|x_i\rangle$ ($\hat{Q} = 1 - \hat{P}$) yields

$$X|\Delta_i\rangle + \hat{P}\hat{x}\hat{Q}|x_i\rangle = x_i|\Delta_i\rangle \tag{6}$$

where we have used $\hat{P}^2 = \hat{P}$. In the complete basis set limit, $\hat{Q} = 0$, thus $|\Delta_i\rangle$ ($|\phi_i\rangle$) becomes exact eigenstates of the position operator. In practice,

$$X|\Delta_i\rangle \simeq x_i|\Delta_i\rangle \tag{7}$$

It is not straightforward to find a DVR set satisfying strictly eq 3. A convenient way to construct a DVR basis set is to diagonalize the X matrix under a finite basis representation although they may not strictly satisfy eq 3.

An important property of DVR basis sets is that matrix elements for coordinate-dependent operators $\hat{O}(x)$ (e.g., potential energy operator) can be simply computed by a diagonal approximation without quadrature

$$O_{ij} = \langle \phi_i|O(\hat{x})|\phi_j\rangle \simeq \delta_{ij}O(x_j) \tag{8}$$

For any state $|\psi\rangle = \sum_{i=1}^{N} c_i|\phi_i\rangle$, the expansion coefficients can be simply obtained by left multiplying $\langle x_j|$ and using eq 3, leading to

$$c_j = w_j^{-1/2}\psi(x_j) \tag{9}$$

Moreover, the kinetic energy operator matrix elements can be computed exactly, instead of using a finite-difference method which requires a dense uniform grid.

A straightforward way to construct a multidimensional DVR is by direct product. For example, for $d = 2$,

$$\chi_{\mathbf{i}}(\mathbf{r}) = \phi_{i_1}(x)\phi_{i_2}(y) \tag{10}$$

where $\mathbf{i} = (i_1, i_2)$ and DVR grid $\mathbf{r}_\mathbf{i} = (x_{i_1}, y_{i_2})$.

https://doi.org/10.1021/acs.jctc.5c00029
J. Chem. Theory Comput. 2025, 21, 6793−6800

2.2. Hybrid Gaussian/DVR. In principle, one can discretize the three-dimensional real space by a direct product DVR basis sets. However, one would encounter the singularity of Coulomb potential at nuclear positions, such singular potentials typically do not occur in vibrational problems. To avoid singularities, one can instead choose to discretize one- or two-dimensions and uses e.g., Gaussian basis functions for the rest coordinates. One-dimensional discretization, leads to sliced basis set,[24] that are particularly convenient for chain-like molecules and for DMRG algorithm. Two-dimensional discretizations are less explored.

Here we focus on the 1D discretization (say z), and use Gaussian basis sets for the transversal plane $\boldsymbol{\rho} = (x, y)$. The exponents of the Gaussians are taken from the Pople basis sets,

$$\chi_i(\boldsymbol{\rho}) = \sqrt{\frac{2\alpha_i}{\pi}}\, e^{-\alpha_i \|\rho-\rho_i\|^2} \tag{11}$$

where $\boldsymbol{\rho}_i$ is the center.

Here we choose the transversal basis set as the eigenstates of the transversal core Hamiltonian.

$$\mathbf{h}(z_n)|\phi_{n\alpha}\rangle = \varepsilon_{n\alpha}|\phi_{n\alpha}\rangle \tag{12}$$

where $\mathbf{h}(z_n) = T_\perp + V(z_n)$ is the transversal single-electron core Hamiltonian matrix represented in the 2D primitive Gaussian bases for the nth slice, and $\varepsilon_{n\alpha}$ is the αth orbital energy. The core Hamiltonian, unlike the Fock Hamiltonian, consists only of the transversal kinetic energy $T_\perp$ and electron−nuclear attraction $V(z_n)$. It parametrically depends on the z coordinate due to the electron−nuclear attraction. The advantage of such transversal basis sets is that for noncollinear chain-like molecules it can adapt to the local electric potential and reduce the number of transversal orbitals.

We compare the contracted and uncontracted basis sets for the hydrogen atom. We choose $N_z = 256$ grid points in the range $(-6, 6)$ a_0 and with the minimal STO-6G basis (i.e., $N_o = 6$). The contracted Gaussian basis sets are obtained simply by slicing the STO-6G basis. That is, the transversal orbital for nth slice is given by

$$\phi_n(\boldsymbol{\rho}) = \mathcal{N}_n \sum_{i=1}^{6} C_i \chi_i(\boldsymbol{\rho}; z_n) \tag{13}$$

where $\chi_i(\mathbf{r})$ is the primitive Gaussian bases used in STO-6G with C_i the contraction coefficients, and $\mathcal{N}_n$ is the renormalization constant. The ground state energy with the contracted basis set is -0.4776 E_h (exact value is -0.5 E_h). Treating the six projected Gaussian functions $\{\chi_i(\boldsymbol{\rho})\}$ as independent, the ground state energy with the transversal core orbitals is improved to -0.4994 E_h. Note that the projected Gaussian basis functions are independent of z upon renormalization.

2.3. DMRG/DVR. Quantum chemistry computations starts with building the one- and two-electron integrals in a chosen basis set. The full basis set (atomic orbital) is given by

$$|\psi_{ni}\rangle = |\phi_{ni}\rangle \otimes |z_n\rangle \tag{14}$$

where $|\phi_{ni}\rangle$ is the ith transversal orbital at the nth slice and $|z_n\rangle$ denotes the nth DVR basis function. The number of DMRG sites $L = N_z \times N_o$ is determined by the number of DVR slices N_z and the number of transversal orbitals for each slice N_o. With a DVR basis set, the kinetic energy operator in z-direction $\hat{T}_z = -\frac{1}{2}\nabla_z^2$ can be computed exactly, whereas a dense grid is required in finite-difference methods to have good accuracy.

The core Hamiltonian matrix elements are given by

$$\langle\psi_{ni}|\hat{T}_z + \mathbf{h}(z)|\psi_{n'j}\rangle = \delta_{nn'}\delta_{ij}\varepsilon_{ni} + T^z_{nn'}S_{ni,n'j} \equiv h_{ni,n'j} \tag{15}$$

where $S_{ni,n'j} = \langle\phi_{ni}|\phi_{n'j}\rangle = \int d^2\boldsymbol{\rho}\phi^*_{ni}(\boldsymbol{\rho})\phi_{n'j}(\boldsymbol{\rho})$ is the overlap matrix between transversal basis sets at different slices.

Both the one-electron integrals (including the overlap matrix, kinetic energy operator, and electron−nuclear attraction) and the two-electron integrals (i.e., the electron repulsion integrals)

$$v^{nn'}_{ijkl} = \iint d^2\boldsymbol{\rho}_1 d^2\boldsymbol{\rho}_2 \frac{\phi^n_i(\boldsymbol{\rho}_1)\phi^{n'}_j(\boldsymbol{\rho}_2)\phi^{n'}_k(\boldsymbol{\rho}_2)\phi^n_l(\boldsymbol{\rho}_1)}{\sqrt{|\boldsymbol{\rho}_1 - \boldsymbol{\rho}_2|^2 + (z_n - z_{n'})^2}} \tag{16}$$

can be analytically calculated, see App. A for details.

Thus, the electronic Hamiltonian in the second-quantized form is given by

$$H = \sum_{n,n'}\sum_{\sigma} h_{ni,n'j}c^\dagger_{ni\sigma}c_{n'j\sigma} + \frac{1}{2}\sum_{\sigma,\tau}\sum_{i,j,k,l=1}^{N_o} v^{nn'}_{ijkl}c^\dagger_{ni\sigma}c^\dagger_{n'j\tau}c_{n'k\tau}c_{nl\sigma} + V_{NN}$$

where V_{NN} is the nuclear repulsion energy and $\sigma, \tau = \{\uparrow, \downarrow\}$, $c_{ni\sigma}$ ($c^\dagger_{ni\sigma}$) annihilates (creates) an spin-σ electron at i-th transversal orbital of the nth slice. The electron operators satisfy the canonical anticommutation relations $\{c_{ni\sigma}, c^\dagger_{n'j\tau}\} = c_{ni\sigma}c^\dagger_{n'j\tau} + c^\dagger_{n'j\tau}c_{ni\sigma} = \delta_{nn'}\delta_{ij}\delta_{\sigma\tau}$, $\{c_{ni\sigma}, c_{n'j\tau}\} = 0$.

The electronic Hamiltonian is mapped to an interacting spin model by the Jordan-Wigner transformation.[29] This transformation is also widely used to map an electronic structure problem onto a quantum computer.[30] For spinful electrons, the transformation reads

$$\begin{aligned}
c_{\uparrow,j} &\leftrightarrow (-1)^{\sum_{l<j} n_{\uparrow,l}+n_{\downarrow,l}}\sigma^-_{\uparrow,j},\\
c^\dagger_{\uparrow,j} &\leftrightarrow (-1)^{\sum_{l<j} n_{\uparrow,l}+n_{\downarrow,l}}\sigma^+_{\uparrow,j},\\
c_{\downarrow,j} &\leftrightarrow (-1)^{\sum_{l<j} n_{\uparrow,l}+n_{\downarrow,l}}(-1)^{n_{\uparrow,j}}\sigma^-_{\downarrow,j},\\
c^\dagger_{\downarrow,j} &\leftrightarrow (-1)^{\sum_{l<j} n_{\uparrow,l}+n_{\downarrow,l}}(-1)^{n_{\uparrow,j}}\sigma^+_{\downarrow,j}
\end{aligned} \tag{17}$$

$\sigma^\pm_{\uparrow,j}$, $\sigma^\pm_{\downarrow,j}$ are the spin-1/2 Pauli matrices at jth site. For a single spin-orbital site in the $\{|0\rangle, |\uparrow\rangle, |\downarrow\rangle, |\uparrow\downarrow\rangle\}$ basis,

$$\sigma_\uparrow = \begin{bmatrix} 0 & 0 & 1 & 0\\ 0 & 0 & 0 & 1\\ 0 & 0 & 0 & 0\\ 0 & 0 & 0 & 0 \end{bmatrix},\quad \sigma_\downarrow = \begin{bmatrix} 0 & 1 & 0 & 0\\ 0 & 0 & 0 & 0\\ 0 & 0 & 0 & -1\\ 0 & 0 & 0 & 0 \end{bmatrix} \tag{18}$$

As the creation and annihilation operators always appear in pairs in the Hamiltonian, it is useful to note that $n_{\uparrow,j} \leftrightarrow \frac{1}{2}(1 + \sigma^z_{\uparrow,j})$, $n_{\downarrow,j} \leftrightarrow \frac{1}{2}(1 + \sigma^z_{\downarrow,j})$.

For the Jordan-Wigner transformed Hamiltonian, a many-spin eigenstate can be expressed as

$$|\Psi\rangle = \sum_{\boldsymbol{\sigma}} C_{\sigma_1\sigma_2\cdots\sigma_L}|\sigma_1\sigma_2\cdots\sigma_L\rangle \tag{19}$$

where L is the number of orbitals in the active space, $|\sigma_l\rangle = \{|0\rangle, |\uparrow\rangle, |\downarrow\rangle, |\uparrow\downarrow\rangle\}$.

https://doi.org/10.1021/acs.jctc.5c00029
J. Chem. Theory Comput. 2025, 21, 6793−6800

In DMRG, the high-dimensional coefficients (of size 4^L) is approximated by a MPS,

$$C_{\boldsymbol{\sigma}} = \sum_{\boldsymbol{\alpha}} M^{[1]\sigma_1}_{1\alpha_1} M^{[2]\sigma_2}_{\alpha_1\alpha_2} \cdots M^{[L]\sigma_L}_{\alpha_{L-1}1} \tag{20}$$

where $M^{[i]\sigma_i}_{\alpha_{i-1}\alpha_i}$ is a tensor with one index σ_n representing the physical states and two virtual bond indices α_i. In practical implementations the bond dimension is restricted to be smaller than a maximum D.

The DMRG calculation can be either carried out in the original algorithm[20] or the matrix product operator/matrix product state (MPO/MPS) framework.[21] We have implemented both schemes for the pseudo-hydrogen model system and used the MPO/MPS for realistic molecules.

The main steps for the conventional DMRG algorithm are sketched below.

1. We first create electronic DVR basis sets $\{|\phi_j\rangle, j = 1, 2,..., L\}$. Here we use sine DVR.
2. The DMRG calculation is initiated by the infinite DMRG algorithm. For each step, the system block is enlarged by one more site, the Hamiltonian of l+1 sites is represented in terms of $\{|\psi_n^{0,...,l-1}\rangle \otimes |\sigma_l\rangle, n = 0, 1,..., D - 1\}$. Similarly for the environment block. Build the entire superblock Hamiltonian of $2(l+1)$ sites in terms of $\{|\psi_n^{0,...,l-1}\rangle \otimes |\sigma_l\rangle \otimes |\sigma_{l+1}\rangle \otimes |\psi_m^{l+1,..., 2l+1}\rangle\}$.
3. Compute the ground state energy and eigenstate of the entire system by e.g., Lanczos algorithm, compute the reduced density matrix followed by Schmidt decomposition (i.e., singular value decomposition), retain D eigenvectors with largest Schmidt coefficients. The same is applied for the environment block. Then, the system-environment interaction operators is updated with the new bases.
4. When the entire system reaches the desired length L (i.e., number of DVR set), we start the sweeping algorithm. During the sweep, the system block grows at the expense of the environment block, with the total number of sites (orbitals) conserved.

For the conventional DMRG algorithm, we fix the number of electrons by an energy penalty

$$\begin{aligned} H_N &= \mu(\hat{N} - N)^2 \\ &= \mu \sum_{i,j} n_i n_j - 2\mu N \sum_i n_i + \mu N^2 \end{aligned} \tag{21}$$

where $\hat{N} = \sum_{i=1}^{L} n_i$ is the total number operator. Nevertheless, in the MPO/MPS implementation, we exploit two U(1) symmetry corresponding to the conservation of electron number and spin magnetic quantum number. The algorithm used to enforce U(1) symmetry follows the same approach as for canonical molecular orbitals.[42] The reduced density matrix is block-diagonal with respect to the quantum numbers, and renormalization is performed only within each symmetry block.

For the MPS implementation, the electronic Hamiltonian is first represented in a MPO form using the bipartite graph algorithm in ref 31 and the MPS is then optimized recursively.

3. RESULTS

We first consider a one-dimensional pseudo-hydrogen chain model with screened Coulomb interaction.[37] The electronic Hamiltonian reads

$$H(\mathbf{z}) = \sum_{i=1}^{N_e} -\frac{1}{2}\nabla_i^2 + v_{ee} + v_{en}(\mathbf{z}) + v_{nn}(\mathbf{z}) \tag{22}$$

where $\mathbf{z}$ is the proton positions along the chain. We use the regularized Coulomb interaction

$$v_C(r) = \frac{\mathrm{erf}(r)}{r} \tag{23}$$

This model mimics a single transversal basis limit of the sliced basis DMRG.[24]

For comparison, we also computed the ground state energy of a one-dimensional pseudo-hydrogen chain using the complete active space configuration interaction (CASCI) method with canonical molecular orbitals. The same DVR basis set is used as the primitive basis. The canonical molecular orbitals are obtained by a HF/DVR calculation (App. B) followed by a CASCI calculation (implementation details shown in App. C).

We use the sine DVR with grid points uniformly distributed in the range of (−15, 15) Å. The boundary points are not included as the open boundary condition is imposed, i.e., $\phi(x_{min}) = \phi(x_{max}) = 0$. For the DMRG, there is no need for the HF calculation here since we directly use eigenstates of the core Hamiltonian instead of the Fock Hamiltonian as the transversal orbitals.

For the molecular geometry is $\mathbf{z}_0 = [-L/2, -L/6, L/6, L/2]$, L = 10 Å, the ground state energies are shown in Table 1. The DMRG total energy with D = 12 matches the CASCI energy with 12 active orbitals up to 0.1 mE_h.

Table 1. Energies of DMRG/DVR and CASCI(n_o, n_e)/DVR with Different Sizes of Basis Sets for a 1D Pseudo-Hydrogen Chain[a]

L	method	energy (E_h)
32	HF	−1.412298
32	CASCI(6, 4)	−1.423990
32	CASCI(12, 4)	−1.425417
32	DMRG (D = 10)	−1.424155
32	DMRG (D = 12)	−1.425322

[a] D is the maximum number of states retained in DMRG, i.e., bond dimension in the language of matrix product states.

For the realistic hydrogen chain H_n, to benchmark the accuracy of the DMRG/DVR method, we compare the DMRG/DVR ground state energies with HF, CCSD, and FCI using conventional Pople basis set varying the number of hydrogen atoms n and the bond dimension D. The results are shown in Figure 1. A more fair comparison should be using the same basis set for all methods, but that is beyond the scope of this work. Comparing the HF and FCI energies, the correlation energy in the hydrogen chain is approximately 0.02 E_h per atom. The CCSD results are in good agreement with FCI. For n = 4, 6 hydrogen atoms the DMRG/DVR energies are found to be lower than the FCI/6−31G energies. The FCI is limited to 6 hydrogen atoms using a single CPU due to the exponential grow of computational cost with the number of orbitals, whereas DMRG can treat systems beyond reach of traditional FCI implementations (96 orbitals here, N_z = 32, N_o = 3). The FCI computations are performed using PySCF.[38]

To show the advantages of DVR basis sets, Figure 2 shows the convergence of DMRG with the bond dimension D for H_4.

https://doi.org/10.1021/acs.jctc.5c00029
J. Chem. Theory Comput. 2025, 21, 6793−6800

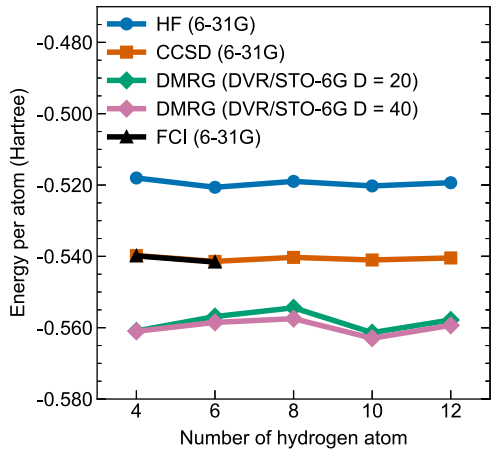

Figure 1. Comparison of the ground state energies for varying lengths of hydrogen chain between DMRG/DVR and HF, CCSD, and FCI using conventional Pople basis set. The FCI method is limited to n = 6 due to the large computational cost. CCSD: Coupled cluster singlet-doublet. FCI: Full configuration interaction. HF: Hartree−Fock. DMRG: Density matrix renormalization group. DVR: Discrete variable representation.

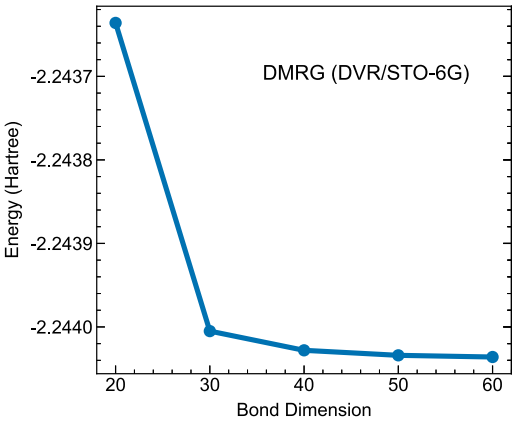

Figure 2. Convergence of DMRG energy with bond dimension for H_4 at $\mathbf{z}$ = (−3.6, −1.1667, 1.1667, 3.6) a_0. The number of DMRG sites is 96.

The ground state energy converges quickly at D = 40 up to 0.1 mE_h reflecting the limited orbital entanglement in the DVR sites. Increasing the bond dimension D from 20 to 40, the DMRG energy only changes by 0.001 E_h per atom except for n = 8 where the difference is slightly higher 0.003 E_h. In Table 2, we used a larger basis set (6−311G**) for FCI for two configurations of H_4, the DMRG/DVR energies lie in between the FCI/6−31G and FCI/6−311G**.

4. SUMMARY

We have developed an implementation of the DMRG and CASCI using a hybrid Gaussian/DVR basis set. The electron repulsion integrals can be easily computed and scales linearly with the number of DVR basis functions. The DMRG and CASCI with DVR basis sets are first applied to a one-dimensional pseudo-hydrogen chain model with screened Coulomb interaction and then to a realistic hydrogen chain. For the model system, the DMRG results with a small bond dimension agrees with the CASCI results up to 0.1 mE_h. For realistic H_n, the accuracy of DMRG/DVR energy with a small bond dimension is in general comparable to the FCI energy with Pople basis set. While we have only used s-type orbitals for the hydrogen chain, it is straightforward to include p-type orbitals in our method since the required matrix elements can be analytically obtained.

Table 2. Energies for Realistic Hydrogen Chain H_4 at $\mathbf{z}_1$ = (−3.6, −1.1667, 1.1667, 3.6) and $\mathbf{z}_2$ = (−3.6, −0.91, 0.91, 3.6) a_0[a]

method	$E(\mathbf{z}_1)$	$E(\mathbf{z}_2)$
HF/STO-6G	−1.967556	−2.050585
FCI/STO-6G	−2.084897	−2.143138
FCI/631G	−2.159435	−2.200606
FCI/6311G**	−2.185384	−2.227971
DMRG (D = 20)	−2.174086	−2.241739
DMRG (D = 40)	−2.176288	−2.243043

[a]In DMRG/DVR, N_z = 32, N_o = 3. The exponents of the primitive transversal Gaussian basis functions are extracted from the STO-6G basis set.

These results demonstrate the utility of the hybrid Gaussian/DVR basis sets in DMRG and multiconfigurational electronic structure methods. Specifically, the DVR basis sets can reduce orbital entanglement enhancing the convergence of DMRG method. The use of nonatom-centered primitive basis sets significantly simplifies the computation of many-electron wave function overlap, which has been shown to account for all nonadiabatic effects.[13−15,39] Thus, the DMRG/DVR electronic structure method can be directly integrated with the discrete variable local diabatic representation method to model strongly correlated electron−nuclear dynamics. For nonlinear molecules, in principle, the DMRG/DVR method can be similarly applied if a proper z-axis is chosen using off-centered 2D Gaussians. There is a technical challenge in constructing the analytical expressions for the Coulomb integrals using atom-centered Gaussians. One possibility is to compute such integrals numerically as in ref 24, then our method can be applied to nonlinear molecules in the same way as the chain molecules. It is also interesting to compare the DMRG/DVR method to the sliced basis DMRG with gausslets.[26] We will explore these directions in the future.

APPENDIX

A. One- and Two-Electron Integrals

We use two-dimensional Gaussian basis for the transversal plane $\boldsymbol{\rho} = (x, y)$

$$\chi_i(\boldsymbol{\rho}) = \sqrt{\frac{2\alpha_i}{\pi}}\, e^{-\alpha_i \|\boldsymbol{\rho}-\boldsymbol{\rho}_i\|^2} \tag{24}$$

where α_i is the width and $\boldsymbol{\rho}_i$ is the center. The overlap integrals between transversal Gaussian basis functions are

$$S_{ij} = \langle \chi_i | \chi_j \rangle = \frac{2\sqrt{\alpha_i\alpha_j}}{\alpha_i + \alpha_j} e^{-\frac{\alpha_i\alpha_j}{\alpha_i+\alpha_j}\|\boldsymbol{\rho}_i-\boldsymbol{\rho}_j\|^2} \tag{25}$$

For chain molecules, we choose the center for all Gaussians at (0,0). The transversal kinetic energy matrix elements are

$$T_{ij}^{\perp} = \langle \chi_i | \hat{T}_{\perp} | \chi_j \rangle = \frac{4(\alpha_i\alpha_j)^{3/2}}{(\alpha_i + \alpha_j)^2} \tag{26}$$

The electron-nuclear attraction

https://doi.org/10.1021/acs.jctc.5c00029
J. Chem. Theory Comput. 2025, 21, 6793−6800

$$V_{ij} = \sum_I -\langle \chi_i \left| \frac{Z_I}{\sqrt{\rho^2 + (z - z_I)^2}} \right| \chi_j \rangle = -Z_I v_{ij}(z - z_I) \tag{27}$$

with

$$\begin{aligned} v_{ij}(z) &= -\sqrt{\frac{2\alpha_i}{\pi}}\sqrt{\frac{2\alpha_j}{\pi}} \iint \mathrm{d}x\mathrm{d}y \frac{e^{-\alpha_{ij}\rho^2}}{\sqrt{\rho^2 + z^2}} \\ &= -\sqrt{\frac{2\alpha_i}{\pi}}\sqrt{\frac{2\alpha_j}{\pi}} \int_0^\infty 2\pi\rho\mathrm{d}\rho \frac{e^{-\alpha_{ij}\rho^2}}{\sqrt{\rho^2 + z^2}} \\ &= -2\pi^{1/2}\sqrt{\frac{\alpha_i\alpha_j}{\alpha_{ij}}} e^{\alpha_{ij}z^2} \mathrm{erfc}(\sqrt{\alpha_{ij}}|z|) \end{aligned} \tag{28}$$

where $\alpha_{ij} = \alpha_i + \alpha_j$. To avoid numerical difficulty with large variables in erfc(x), when $x > 9$, we use an expansion

$$\mathrm{erfc}(x) \approx (a_1 t + a_2 t^2 + \ldots + a_5 t^5) e^{-x^2} \tag{29}$$

where $t = (1 + \kappa x)^{-1}$, $\kappa = 0.3275911$, $a_1 = 0.254829592$, $a_2 = -0.284496736$, $a_3 = 1.421413741$, $a_4 = -1.453152027$, $a_5 = 1.061405429$.

A.1. Electron Repulsion Integral

The two-electron repulsion integral $v_{ijkl}^{nn'} = \sqrt{\frac{2\alpha_i}{\pi}}\sqrt{\frac{2\alpha_j}{\pi}}\sqrt{\frac{2\alpha_k}{\pi}}\sqrt{\frac{2\alpha_l}{\pi}} V_0$,

$$V_0 = \int \mathrm{d}^2\boldsymbol{\rho}_1 \mathrm{d}^2\boldsymbol{\rho}_2 \frac{e^{-\alpha_{ij}\rho_1^2 - \alpha_{kl}\rho_2^2}}{\sqrt{\|\boldsymbol{\rho}_1 - \boldsymbol{\rho}_2\|^2 + z_{nn'}^2}} \tag{30}$$

where $z_{nn'} = z_n - z_{n'}$, $\rho_i = \|\boldsymbol{\rho}_i\|$. Inserting the Fourier transformation of a Gaussian $e^{-\alpha_{ij}\rho_1^2} = \frac{\pi}{\alpha_{ij}} \int \frac{\mathrm{d}^2\mathbf{k}}{(2\pi)^2} \exp\left(-\frac{k^2}{4\alpha_{ij}}\right) e^{-i\mathbf{k}\cdot\boldsymbol{\rho}_1}$ and of the Coulomb interaction

$$\frac{1}{\sqrt{\rho^2 + z_{nn'}^2}} = \int \frac{\mathrm{d}^2\mathbf{k}}{(2\pi)^2} \frac{2\pi}{k} e^{-kz_{nn'}} e^{-i\mathbf{k}\cdot\boldsymbol{\rho}} \tag{31}$$

into eq 30 leads to

$$\begin{aligned} V_0 = \frac{\pi^2}{\alpha_{ij}\alpha_{kl}} \int \mathrm{d}^2\boldsymbol{\rho}_1 \mathrm{d}^2\boldsymbol{\rho}_2 \frac{\mathrm{d}^2\mathbf{k}_1}{(2\pi)^2} \frac{\mathrm{d}^2\mathbf{k}_2}{(2\pi)^2} \frac{\mathrm{d}^2\mathbf{k}_3}{(2\pi)^2} \times \frac{2\pi}{k_2} e^{-k_2 z_{nn'}} \\ e^{-i\mathbf{k}_2\cdot(\boldsymbol{\rho}_1 - \boldsymbol{\rho}_2)} \times e^{-k_1^2/4\alpha_{ij}} e^{-i\mathbf{k}_1\cdot\boldsymbol{\rho}_1} e^{-k_3^2/4\alpha_{kl}} e^{-i\mathbf{k}_3\cdot\boldsymbol{\rho}_2} \end{aligned} \tag{32}$$

Upon integration over $\boldsymbol{\rho}_1$ and $\boldsymbol{\rho}_2$ yields

$$V_0 = \frac{\pi^2}{\alpha_{ij}\alpha_{kl}} \int \frac{\mathrm{d}^2\mathbf{k}}{(2\pi)^2} \frac{2\pi}{k} e^{-kz_{nn'}} e^{-(\alpha_{ij} + \alpha_{kl})/\left(4\alpha_{ij}\alpha_{kl}\right)k^2} \tag{33}$$

It follows that

$$\begin{aligned} V_0 &= \frac{\pi^2}{\alpha_{ij}\alpha_{kl}} \int_0^{2\pi} \mathrm{d}\theta \int_0^\infty \frac{k\mathrm{d}k}{2\pi k} e^{-kz_{nn'} - (\alpha_{ij} + \alpha_{kl})/\left(4\alpha_{ij}\alpha_{kl}\right)k^2} \\ &= \frac{e^{\mathcal{Z}^2}\pi^{5/2}\mathrm{erfc}(\mathcal{Z})}{\sqrt{\alpha_{ij}\alpha_{kl}(\alpha_{ij} + \alpha_{kl})}} \end{aligned} \tag{34}$$

where $\mathcal{Z} = \sqrt{\alpha_{ij}\alpha_{kl}z_{nn'}^2/(\alpha_{ij} + \alpha_{kl})}$ and

$$v_{ijkl}^{nn'} = 4\sqrt{\alpha_i\alpha_j\alpha_k\alpha_l} \frac{e^{\mathcal{Z}^2}\pi^{1/2}\mathrm{erfc}(\mathcal{Z})}{\sqrt{\alpha_{ij}\alpha_{kl}(\alpha_{ij} + \alpha_{kl})}} \tag{35}$$

B. Hartree–Fock/DVR

For comparison, we also implemented the CASCI using DVR basis set. The active space is defined by the HF canonical molecular orbitals (MOs). In the restricted HF theory, the many-electron wave function is approximated by a single Slater determinant (closed shell)

$$|\Phi_0\rangle = |\psi_1\overline{\psi}_1 \cdots \psi_{n_e/2}\overline{\psi}_{n_e/2}| \tag{36}$$

where $\psi_p(\overline{\psi}_p)$ denotes, respectively, molecular orbitals with spin up (down), n_e is the number of electrons. The MOs are expanded using the DVR basis set,

$$\psi_n(\mathbf{r}) = \sum_{\mathbf{i}} \chi_{\mathbf{i}}(\mathbf{r}) C_{\mathbf{i},n} \tag{37}$$

The optimal molecular orbitals minimizing the total energy are obtained by diagonalizing the Fock matrix

$$\mathbf{F}[\mathbf{C}] = \mathbf{h} + 2\mathbf{J} - \mathbf{K} \tag{38}$$

where

$$h_{\mathbf{ij}} = \langle \chi_{\mathbf{i}}| -\frac{1}{2}\Delta + v_{\mathrm{en}}(\mathbf{R})|\chi_{\mathbf{j}}\rangle = t_{\mathbf{ij}} + \delta_{\mathbf{ij}}v_{\mathbf{i}} \tag{39}$$

is the DVR core Hamiltonian consisting of the kinetic energy and electron-nuclear interaction, $t_{\mathbf{ij}} = \langle \chi_{\mathbf{i}}| -\frac{1}{2}\Delta|\chi_{\mathbf{j}}\rangle$ is the DVR kinetic energy matrix elements, Δ is the Laplacian in d-dimensions.

The Hartree potential

$$J_{\mathbf{ij}} = \delta_{\mathbf{ij}} \sum_k v_{\mathbf{ik}} D_{\mathbf{kk}} \tag{40}$$

is diagonal in the DVR set, and the exchange

$$K_{\mathbf{ij}} = v_{\mathbf{ij}} D_{\mathbf{ij}} \tag{41}$$

Here $D_{\mathbf{ij}} = \langle \Psi_0|c_{\mathbf{j}}^\dagger c_{\mathbf{i}}|\Psi_0\rangle$ is the DVR one-electron reduced density matrix, and $v_{\mathbf{ij}} = (\mathbf{ii}|\mathbf{jj})$ is the electron repulsion. The HF/DVR calculation scales linearly with the number of basis functions N.

C. CASCI/DVR

CASCI is a full configuration-interaction computation in a chosen subset of single-electron orbitals, i.e., the complete active space. The orbitals can be the canonical molecular orbitals defined in the HF theory, or natural orbitals defined as the eigenstates of the one-electron reduced density matrix. Upon the convergence of the self-consistent field cycle, the electronic Hamiltonian can be transformed from DVR set to MOs,

$$H = \sum_{p,q} \sum_{\sigma=\uparrow,\downarrow} h_{pq} c_{p\sigma}^\dagger c_{q\sigma} + \sum_{p,q,r,s} \sum_{\sigma,\tau=\uparrow,\downarrow} \frac{1}{2}(pq|rs) c_{p\sigma}^\dagger c_{r\tau}^\dagger c_{s\tau} c_{q\sigma} \tag{42}$$

where p, q, r, s labels the generic molecular orbitals. The MO electron repulsion integrals in eq 42 can be obtained by

$$(pr|qs) = \sum_{\mathbf{i},\mathbf{j}} U_{\mathbf{ip}} U_{\mathbf{jq}} U_{\mathbf{ir}} U_{\mathbf{js}} v_{\mathbf{ij}} \tag{43}$$

where U is the transformation matrix from DVR set to MOs.

https://doi.org/10.1021/acs.jctc.5c00029
J. Chem. Theory Comput. 2025, 21, 6793−6800

The CASCI computation can proceed by building a full configuration interaction Hamiltonian within the Slater determinants or configuration state functions corresponding to all possible excitations in the active space.[32] Slater determinants are chosen here as it simplifies the implementation,[33]

$$|\Psi_\alpha\rangle = \sum_I c_I^\alpha |\Phi_I\rangle \tag{44}$$

and the configuration intersection coefficients $\mathbf{c}^\alpha$ are obtained by diagonalization,

$$\mathbf{H}\mathbf{c}^\alpha = E_\alpha \mathbf{c}^\alpha \tag{45}$$

Each electronic configuration, or Slater determinant, is labeled a binary array $B^I_{p\sigma}$, where p labels the orbital, $\sigma = \uparrow, \downarrow$ is the spin index, and I labels the Slater determinant.[34] The matrix elements between determinants $\langle\Phi_J|H|\Phi_I\rangle$ are computed by the Slater-Condon rules.[35,36] The full configuration interaction method uses all MOs to build Slater determinants. This is impractical as the computational cost scales exponentially with the number of orbitals. The active space is usually a subset of the MOs with the doubly occupied core orbitals frozen. The energy of the frozen core electrons is the same as a closed-shell molecule

$$E_{\mathrm{FC}} = 2\sum_{f\in \mathrm{FC}} h_{ff} + \sum_{f,g} 2J_{fg} - K_{fg} \tag{46}$$

The interaction between the active space and frozen core orbitals reads

$$V_{\text{AS-FC}} = \sum_\sigma \sum_{i,j\in \mathrm{AS}} \sum_{k\in \mathrm{FC}} (2(ij|kk) - (ik|kj)) c^\dagger_{i\sigma} c_{j\sigma} \tag{47}$$

where i, j refers to orbitals in the active space and k the frozen core orbitals. The second-quantized Hamiltonian in the active space reads

$$H_{\mathrm{AS}} = E_{\mathrm{FC}} + \sum_{i,j}\sum_\sigma \tilde{h}_{ij} c^\dagger_{i\sigma} c_{j\sigma} + \sum_{i,j,k,l}\sum_{\sigma,\tau=\uparrow,\downarrow} \frac{1}{2}(ij|kl)\, c^\dagger_{i\sigma} c^\dagger_{k\tau} c_{l\tau} c_{j\sigma} \tag{48}$$

where $\tilde{h}_{ij} = h_{ij} + \sum_{k\in \mathrm{FC}} 2(ij|kk) - (ik|kj)$.

C.1. Implementation Details

The main steps for implementing the CASCI with DVR basis sets are as follows

1. We first create electronic DVR basis sets $\{|\chi_{\mathbf{j}}\rangle\}$, labeled by $\mathbf{j} = (n_1, \ldots, n_d)$ where d is the dimensionality of real-space.
2. Perform mean-field HF calculation to yield MOs

$$|\phi_p\rangle = \sum_{\mathbf{j}} |\chi_{\mathbf{j}}\rangle U_{\mathbf{j}p} \tag{49}$$

and orbital energies ε_p. The DVR to MO transformation is used to transform the creation and annihilation operators,

$$c^\dagger_p = \sum_{\mathbf{j}} U_{\mathbf{j}p} c^\dagger_{\mathbf{j}}, \quad c^\dagger_{\mathbf{j}} = \sum_p [U^\dagger]_{p\mathbf{j}} c_p\dagger \tag{50}$$

The HF self-consistent field computations are similar to the standard Gaussian-type orbital-based computations,[1,40] the only difference is that the one-electron and two-electron integrals are straightforwardly evaluated in the DVR basis set. For spin-unrestricted calculations,

$$\phi_{p\sigma}(\mathbf{r}) = \sum_{\mathbf{i}} C^\sigma_{\mathbf{i}p}\chi_{\mathbf{i}}(\mathbf{r}) \tag{51}$$

3. Fill electrons according to the Aufbau principle.
4. Choose the active space with L MOs.
5. Transform the electronic Hamiltonian to the second-quantized form in the active space.
6. Build the configuration interaction Hamiltonian. Alternatively, we can also map the electronic Hamiltonian to a spin model by Jordan-Wigner transformation. The transformed Hamiltonian is highly sparse with size 4^L for spin unrestricted calculations as each orbital contains four states $|0\rangle$, $|\uparrow\rangle$, $|\downarrow\rangle$, $|\uparrow\downarrow\rangle$.
7. Use Lanczos or Davidson matrix diagonalization method to obtain low-lying eigenenergies E_α and eigenstates $|\Psi_\alpha\rangle$. When the active space is large $L > 20$, a direct diagonalization is impractical and more efficient methods such as the density matrix renormalization group methods and the iterative configuration intersection can be used.[20,21,41]

AUTHOR INFORMATION

Corresponding Author

Bing Gu − *Department of Chemistry and Department of Physics, Westlake University, Hangzhou, Zhejiang 310030, China; Institute of Natural Sciences, Westlake Institute for Advanced Study, Hangzhou, Zhejiang 310024, China;* orcid.org/0000-0002-5787-3334; Email: gubing@westlake.edu.cn

Authors

Jiajun Ren − *MOE Key Laboratory of Theoretical and Computational Photochemistry, College of Chemistry, Beijing Normal University, Beijing 100875, China;* orcid.org/0000-0002-1508-4943

Junzhe Zhang − *Department of Chemistry and Department of Physics, Westlake University, Hangzhou, Zhejiang 310030, China*

Complete contact information is available at: https://pubs.acs.org/10.1021/acs.jctc.5c00029

Notes

The authors declare no competing financial interest.

ACKNOWLEDGMENTS

This work is supported by the National Natural Science Foundation of China (Grant No. 22473090 and 92356310).

REFERENCES

(1) Szabo, A.; Ostlund, N. S. *Modern Quantum Chemistry: Introduction to Advanced Electronic Structure Theory*; Courier Corporation, 1996.

(2) Lischka, H.; Nachtigallová, D.; Aquino, A. J. A.; Szalay, P. G.; Plasser, F.; Machado, F. B. C.; Barbatti, M. Multireference Approaches for Excited States of Molecules. *Chem. Rev.* **2018**, *118*, 7293.

(3) Helgaker, T.; Larsen, H.; Olsen, J.; Jørgensen, P. Direct optimization of the AO density matrix in Hartree - Fock and Kohn - Sham theories. *Chem. Phys. Lett.* **2000**, *327*, 397.

(4) White, S. R.; Wilkins, J. W.; Teter, M. P. Finite-element method for electronic structure. *Phys. Rev. B* **1989**, *39*, 5819.

(5) Chelikowsky, J. R.; Troullier, N.; Saad, Y. Finite-difference-pseudopotential method: Electronic structure calculations without a basis. *Phys. Rev. Lett.* **1994**, *72*, 1240.
(6) LIPPERT, G.; Lippert, B. G.; HUTTER, J.; Parrinello, J. H. a. M. A hybrid Gaussian and plane wave density functional scheme. *Mol. Phys.* **1997**, *92*, 477.
(7) Liu, Y.; Yarne, D. A.; Tuckerman, M. E. *Ab Initio* molecular dynamics calculations with simple, localized, orthonormal real-space basis sets. *Phys. Rev. B* **2003**, *68*, No. 125110.
(8) Rakhuba, M. V.; Oseledets, I. V. Grid-based electronic structure calculations: The tensor decomposition approach. *J. Comput. Phys.* **2016**, *312*, 19.
(9) Mortensen, J. J.; Larsen, A. H.; Kuisma, M.; Ivanov, A. V.; Taghizadeh, A.; Peterson, A.; Haldar, A.; Dohn, A. O.; Schäfer, C.; Jónsson, E. Ö.; Hermes, E. D.; Nilsson, F. A.; Kastlunger, G.; Levi, G.; Jónsson, H.; Häkkinen, H.; Fojt, J.; Kangsabanik, J.; Sødequist, J.; Lehtomäki, J.; Heske, J.; Enkovaara, J.; Winther, K. T.; Dulak, M.; Melander, M. M.; Ovesen, M.; Louhivuori, M.; Walter, M.; Gjerding, M.; Lopez-Acevedo, O.; Erhart, P.; Warmbier, R.; Würdemann, R.; Kaappa, S.; Latini, S.; Boland, T. M.; Bligaard, T.; Skovhus, T.; Susi, T.; Maxson, T.; Rossi, T.; Chen, X.; Schmerwitz, Y. L. A.; Schiøtz, J.; Olsen, T.; Jacobsen, K. W.; Thygesen, K. S. GPAW: An open Python package for electronic structure calculations. *J. Chem. Phys.* **2024**, *160*, No. 092503.
(10) Kim, J.; Hong, K.; Choi, S.; Hwang, S.-Y.; Youn Kim, W. Configuration interaction singles based on the real-space numerical grid method: Kohn - Sham versus Hartree - Fock orbitals. *Phys. Chem. Chem. Phys.* **2015**, *17*, 31434.
(11) Enkovaara, J.; Rostgaard, C.; Mortensen, J. J.; Chen, J.; Dułak, M.; Dulak, M.; Ferrighi, L.; Gavnholt, J.; Glinsvad, C.; Haikola, V.; Hansen, H.; Kristoffersen, H.; Kuisma, M.; Larsen, A.; Lehtovaara, L.; Ljungberg, M.; Lopez-Acevedo, O.; Moses, P. G.; Ojanen, J.; Ojanen, J.; Olsen, T.; Olsen, T.; Petzold, V. G.; Petzold, V.; Romero, N.; Romero, N. A.; Stausholm-M?ller, J.; Stausholm-Møller, J.; Strange, M.; Strange, M.; Tritsaris, G.; Tritsaris, G. A.; Vanin, M.; Vanin, M.; Walter, M.; Walter, M.; Hammer, B.; Hammer, B.; Hakkinen, H.; Häkkinen, H.; Madsen, G.; Madsen, G. K. H.; Nieminen, R.; Nieminen, R. M.; Nørskov, J. K.; Nørskov, J. K.; Puska, M.; Puska, M.; Rantala, T.; Rantala, T. T.; Schiotz, J.; Schiøtz, J.; Thygesen, K. S.; Thygesen, K. S.; Jacobsen, K. W. Electronic structure calculations with GPAW: A real-space implementation of the projector augmented-wave method. *J. Phys.: Condens. Matter* **2010**, *22*, No. 253202.
(12) Light, J. C.; Carrington, T., Jr. Discrete- Variable Representations and their Utilization. In *Advances in Chemical Physics*; John Wiley & Sons, Ltd, 2000; pp 263−310.
(13) Gu, B. A Discrete-Variable Local Diabatic Representation of Conical Intersection Dynamics. *J. Chem. Theory Comput.* **2023**, *19*, 6557.
(14) Gu, B. Nonadiabatic Conical Intersection Dynamics in the Local Diabatic Representation with Strang Splitting and Fourier Basis. *J. Chem. Theory Comput.* **2024**, *20*, 2711.
(15) Zhu, X.; Gu, B. Making Peace with Random Phases: Ab Initio Conical Intersection Quantum Dynamics in Random Gauges. *J. Phys. Chem. Lett.* **2024**, *15*, 8487.
(16) Littlejohn, R. G.; Cargo, M.; Carrington, T.; Mitchell, K. A.; Poirier, B. A general framework for discrete variable representation basis sets. *J. Chem. Phys.* **2002**, *116*, 8691.
(17) Colbert, D. T.; Miller, W. H. A novel discrete variable representation for quantum mechanical reactive scattering via the S -matrix Kohn method. *J. Chem. Phys.* **1992**, *96*, 1982.
(18) Glaser, N.; Baiardi, A.; Reiher, M. Flexible DMRG-Based Framework for Anharmonic Vibrational Calculations. *J. Chem. Theory Comput.* **2023**, *19*, 9329.
(19) Jones, J. R.; Rouet, F.-H.; Lawler, K. V.; Vecharynski, E.; Ibrahim, K. Z.; Williams, S.; Abeln, B.; Yang, C.; McCurdy, W.; Haxton, D. J.; Li, X. S.; Rescigno, T. N. An efficient basis set representation for calculating electrons in molecules. *Mol. Phys.* **2016**, *114*, 2014.
(20) White, S. R. Density matrix formulation for quantum renormalization groups. *Phys. Rev. Lett.* **1992**, *69*, 2863.
(21) Ma, H.; Schollwöck, U.; Shuai, Z. *Density Matrix Renormalization Group (DMRG)-Based Approaches in Computational Chemistry*, 1st ed.; Elsevier: Cambridge, MA, 2022.
(22) Chan, G. K.-L.; Sharma, S. The Density Matrix Renormalization Group in Quantum Chemistry. *Annu. Rev. Phys. Chem.* **2011**, *62*, 465.
(23) Olivares-Amaya, R.; Hu, W.; Nakatani, N.; Sharma, S.; Yang, J.; Chan, G. K.-L. The ab-initio density matrix renormalization group in practice. *J. Chem. Phys.* **2015**, *142*, No. 034102.
(24) Stoudenmire, E. M.; White, S. R. Sliced Basis Density Matrix Renormalization Group for Electronic Structure. *Phys. Rev. Lett.* **2017**, *119*, No. 046401.
(25) White, S. R.; Stoudenmire, E. M. Multisliced gausslet basis sets for electronic structure. *Phys. Rev. B* **2019**, *99*, No. 081110.
(26) Qiu, Y.; White, S. R. Hybrid gausslet/Gaussian basis sets. *J. Chem. Phys.* **2021**, *155*, No. 184107, DOI: 10.1063/5.0068887.
(27) Levine, B. G.; Durden, A. S.; Esch, M. P.; Liang, F.; Shu, Y. CAS without SCF − Why to use CASCI and where to get the orbitals. *J. Chem. Phys.* **2021**, *154*, No. 090902.
(28) Ren, J.; Li, W.; Jiang, T.; Wang, Y.; Shuai, Z. Time-dependent density matrix renormalization group method for quantum dynamics in complex systems. *Wiley Interdiscip. Rev.: Comput. Mol. Sci.* **2022**, *12*, No. e1614.
(29) Jordan, P.; Wigner, E. On the Paulian prohibition of equivalence. *Z. Physik* **1928**, *47*, 631−651.
(30) McArdle, S.; Endo, S.; Aspuru-Guzik, A.; Benjamin, S. C.; Yuan, X. Quantum computational chemistry. *Rev. Mod. Phys.* **2020**, *92*, No. 015003.
(31) Ren, J.; Li, W.; Jiang, T.; Shuai, Z. A general automatic method for optimal construction of matrix product operators using bipartite graph theory. *J. Chem. Phys.* **2020**, *153*, No. 084118.
(32) Helgaker, T.; Jorgensen, P.; Olsen, J. *Molecular Electronic-Structure Theory*; Wiley, 2014.
(33) Candanedo, J. *Notes on Generalized Configuration-Interaction in python*, American Chemical Society (ACS), 2023.
(34) David Sherrill, C.; Schaefer, H. F. The Configuration Interaction Method: Advances in Highly Correlated Approaches. In *Advances in Quantum Chemistry*; Elsevier, 1999; Vol. *34*, pp 143−269.
(35) Slater, J. C. The Theory of Complex Spectra. *Phys. Rev.* **1929**, *34*, 1293.
(36) Condon, E. U. The Theory of Complex Spectra. *Phys. Rev.* **1930**, *36*, 1121.
(37) Stoudenmire, E. M.; Wagner, L. O.; White, S. R.; Burke, K. One- Dimensional Continuum Electronic Structure with the Density-Matrix Renormalization Group and Its Implications for Density-Functional Theory. *Phys. Rev. Lett.* **2012**, *109*, 056402.
(38) Sun, Q.; Zhang, X.; Banerjee, S.; Bao, P.; Barbry, M.; Blunt, N. S.; Bogdanov, N. A.; Booth, G. H.; Chen, J.; Cui, Z.-H.; Eriksen, J. J.; Gao, Y.; Guo, S.; Hermann, J.; Hermes, M. R.; Koh, K.; Koval, P.; Lehtola, S.; Li, Z.; Liu, J.; Mardirossian, N.; McClain, J. D.; Motta, M.; Mussard, B.; Pham, H. Q.; Pulkin, A.; Purwanto, W.; Robinson, P. J.; Ronca, E.; Sayfutyarova, E.; Scheurer, M.; Schurkus, H. F.; Smith, J. E. T.; Sun, C.; Sun, S.-N.; Upadhyay, S.; Wagner, L. K.; Wang, X.; White, A.; Whitfield, J. D.; Williamson, M. J.; Wouters, S.; Yang, J.; Yu, J. M.; Zhu, T.; Berkelbach, T. C.; Sharma, S.; Sokolov, A.; Chan, G. K.-L. Recent developments in the PySCF program package. *J. Chem. Phys.* **2020**, *153*, No. 024109.
(39) Xie, Y.; Yang, Y.; Zhu, X.; Chen, A.; Gu, B. Nondirect- Product Local Diabatic Representation with Smolyak Sparse Grids. *J. Chem. Theory Comput.* **2024**, *20*, 9512.
(40) Thijssen, J. M. J. M. *Computational Physics*; Cambridge University Press: Cambridge, UK; New York, 2007.
(41) Liu, W.; Hoffmann, M. R. iCI: Iterative CI toward full CI. *J. Chem. Theory Comput.* **2016**, *12*, 1169.
(42) Zgid, D.; Nooijen, M. On the spin and symmetry adaptation of the density matrix renormalization group method. *J. Chem. Phys.* **2008**, *128*, No. 014107.